High-bandwidth graded-index polymer optical fibre

Yasuhiro Koike
Faculty of Science and Technology, Keio University, 3-14-1 Hiyoshi, Kohoku-ku, Yokohama 223, Japan
(Received 26 September 1990; revised 18 December 1990; accepted 18 December 1990)

A low-loss and high-bandwidth graded-index (GI) polymer optical fibre in which the attenuation of transmission was less than 150 dB km^{-1} at 650 nm wavelength and the bandwidth was several hundred megahertz kilometres has been successfully obtained by a copolymerization process utilizing the difference of the monomer reactivities. The control of the refractive-index profile and the light scattering of such GI materials are theoretically and experimentally investigated.

(Keywords: optical properties; fibre; light scattering)

INTRODUCTION

Single-mode (SM) glass optical fibres have been widely used as long-distance and high-bandwidth communication media because of their excellent transparency and since it is possible to obtain the necessary precise control of the core diameter. With the spread of fibre-optic technology, new materials have been required to provide the needed properties in practical optical systems. Recently there has been considerable interest in the development of a polymer optical fibre (POF)[1-5] for short-distance communication applications such as local area networks (LANs)[6], datalinks, multinoded bus networks[4], etc., because of its easy processing and handling and its large diameter, enabling high efficiencies of fibre coupling and beam insertion.

In short-distance communication, many junctions and connections of optical fibres would be necessary. In the case of SM optical fibre, the core diameter is about 5 μm, so when connecting two fibres a slight amount of displacement, such as a few micrometres, causes a significant coupling loss. Polymer optical fibre with a large diameter (such as 1 mm) is one of the promising candidates to solve this problem. However, all POFs commercially available[7,8] have been of the step-index (SI) type. Therefore, even in short-range optical communication, the SI POF will not be able to cover the whole bandwidth of the order of hundreds of megahertz that will be necessary in fast datalinks or LANs in the near future, because the bandwidth of the SI POF is only $\sim$5 MHz km.

On the other hand, a graded-index (GI) POF is expected to have a much higher bandwidth than an SI POF, while maintaining a large diameter. The GI POF has been prepared by two technologies, i.e. photocopolymerization[9-11] and interfacial-gel copolymerization[12-14] processes. However, the bandwidth of the GI POF has not been measured and the attenuation has been much larger than that of the SI POF, probably due to large-sized heterogeneities of the order of 100 nm inside the GI core materials. In this paper, a low-loss GI POF with good flexibility was successfully obtained, and evidence of the high bandwidth of GI POF was experimentally confirmed. The formation of the graded index and the optical properties of such a GI POF were described.

PREPARATION OF GRADED-INDEX POLYMER OPTICAL FIBRE

Full details of the photocopolymerization process have been reported elsewhere[9,10], but an outline of the procedure is described here. A mixture of two (M_1 and M_2) or three (M_1, M_2 and M_3) monomers with specified amounts of initiator and chain-transfer agent is placed in a glass tube. Here these monomers have different refractive indices and reactivities. Rotating the tube about its axis, it is exposed to u.v. light passing between the two shades. Meanwhile the u.v. source is moved along the axial direction at a constant velocity. The copolymer phase is initially formed on the inner wall of the glass tube owing to the difference in the u.v. intensity and gradually thickens with irradiation time. Finally the contents of the glass tube are solidified up to the centre axis; this is followed by a sufficient heat treatment.

In the interfacial-gel copolymerization process[12,13], a polymer tube such as poly(methyl methacrylate) (PMMA) is used instead of a glass tube. A monomer mixture, which is essentially the same as in the photocopolymerization process, is placed in a purified polymer tube prepared in our laboratories with outer and inner diameters of 10 mm and 8 mm, respectively. This polymer tube, filled with the monomer mixture, is placed in a furnace at 60–80°C. Here the inner wall of the polymer tube is slightly swollen by the monomer mixture, and a thin gel phase is formed there. Since the rate of the polymerization reaction inside the gel is faster than in the monomer liquid owing to the 'gel effect', polymerization occurs on the inner wall of the tube. The copolymer phase thickens from the periphery to the centre axis of the tube in the same manner as in the photocopolymerization process. U.v. irradiation is also available as an

Paper presented at Speciality Polymers '90, 8–10 August 1990, The Johns Hopkins University, Baltimore, MD, USA

0032-3861/91/101737-09

Table 1 Categories of possible monomers for the photocopolymerization and interfacial-gel copolymerization processes

Group	Monomer		n_D of polymer	Q	e
MA	1. MMA	(methyl methacrylate)	1.49	0.74	0.40
	2. EMA	(ethyl methacrylate)	1.483	0.73	0.52
	3. nPMA	(n-propyl methacrylate)	1.484	0.65	0.44
	4. nBMA	(n-butyl methacrylate)	1.483	0.78	0.51
	5. nHMA	(n-hexyl methacrylate)	1.481	0.67	0.34
	6. iPMA	(isopropyl methacrylate)	1.473	0.85	0.34
	7. iBMA	(isobutyl methacrylate)	1.477	0.72	0.24
	8. tBMA	(t-butyl methacrylate)	1.463	0.76	0.24
	9. CHMA	(cyclohexyl methacrylate)	1.507	0.82	0.45
XMA	10. BzMA	(benzyl methacrylate)	1.568	0.75	0.25
	11. PhMA	(phenyl methacrylate)	1.57	1.49	0.73
	12. 1PhEMA	(1-phenylethyl methacrylate)	1.549	0.74	0.36
	13. 2PhEMA	(2-phenylethyl methacrylate)	1.559	0.74	0.36
	14. FFMA	(furfuryl methacrylate)	1.538	0.78	0.04
A	15. MA	(methyl acrylate)	1.4725	0.42	0.60
	16. EA	(ethyl acrylate)	1.4685	0.52	0.22
	17. BA	(n-butyl acrylate)	1.4634	0.50	1.06
XA	18. BzA	(benzyl acrylate)	1.5584	0.34	0.90
	19. 2ClEA	(2-chloroethyl acrylate)	1.52	0.41	0.54
Ac	20. VAc	(vinyl acetate)	1.47	0.026	−0.22
XAc	21. VB	(vinyl benzoate)	1.578	0.061	−0.55
	22. VPAc	(vinyl phenylacetate)	1.567	0.018	−1.078
	23. VClAc	(vinyl chloroacetate)	1.512	0.074	−0.65
C	24. AN	(acrylonitrile)	1.52	0.60	1.20
	25. αMAN	(α-methylacrylonitrile)	1.52	1.12	0.81
α-A	26. MA(2Cl)	(methyl-α-chloroacrylate)	1.5172	2.02	0.77
	– MAtro	(atropic acid, methyl ester)	1.560	4.78	1.20
St	27. o-ClSt	(*o*-chlorostyrene)	1.6098	1.28	−0.36
	28. p-FSt	(*p*-fluorostyrene)	1.566	0.83	−0.12
	29. o,p-FSt	(*o*,*p*-difluorostyrene)	1.475	0.65	−0.31
	– p-iPSt	(*p*-isopropyl styrene)	1.554	1.60	−1.52

Monomer numbers refer to points in *Figure 1*

energy source for polymerization, but is not necessarily required in this process.

In both processes, the copolymer phase is formed from the inner wall of the tube, while the composition of the copolymer formed during polymerization gradually changes because of the differences in monomer reactivities. Since the refractive indices of the homopolymers are different from one another, a certain kind of radial graded-index profile must be formed.

The resulting GI preform rod was heat-drawn into the GI POF at 230–280°C.

FORMATION OF GRADED INDEX

In the copolymerization reaction between M_i and M_j monomers, the monomer reactivity ratio r_{ij} is defined as:

$$r_{ij} = \frac{k_{ii}}{k_{ij}} \quad \begin{matrix} i = 1, 2, \ldots, n \\ j = 1, 2, \ldots, n \end{matrix} \quad i \neq j \qquad (1)$$

where k_{ij} and k_{ii} are the propagation rate constants in the following copolymerization reactions:

$$\sim\!\sim M_i^{\cdot} + M_i \xrightarrow{k_{ii}} \sim\!\sim M_iM_i^{\cdot}$$

$$\sim\!\sim M_i^{\cdot} + M_j \xrightarrow{k_{ij}} \sim\!\sim M_iM_j^{\cdot}$$

The monomer reactivity ratios r_{ij} and r_{ji} between M_i and M_j monomers are estimated by using equation (2) if the values of Q and e for M_i and M_j monomers are known:

$$\begin{aligned} r_{ij} &= (Q_i/Q_j)\exp[-e_i(e_i - e_j)] \\ r_{ji} &= (Q_j/Q_i)\exp[-e_j(e_j - e_i)] \end{aligned} \qquad (2)$$

Here Q_i (or Q_j) is the reactivity of the monomer M_i (or M_j), and e_i (or e_j) is the electrostatic interaction of the permanent charges on the substituents in polarizing the vinyl group of monomer M_i (or M_j).

Table 1 shows the refractive indices (n_D) of polymers and the Q and e values of about 30 possible monomers for our radical polymerization process. These monomers are categorized into nine groupe as follows: MA, methacrylate group; XMA, methacrylate with high

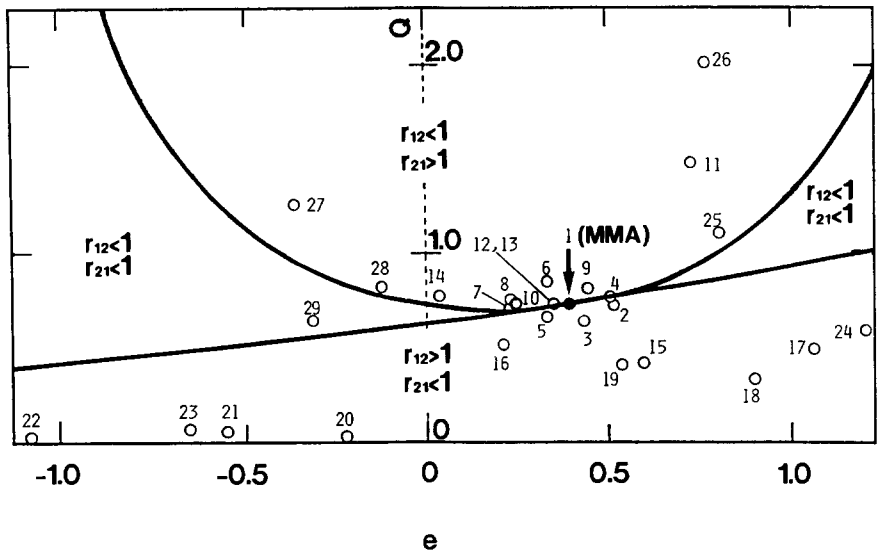

Figure 1 *Q–e* map of monomers in *Table 1*: 1, MMA; 2, EMA; 3, nPMA; 4, nBMA; 5, nHMA; 6, iPMA; 7, iBMA; 8, tBMA; 9, CHMA; 10, BzMA; 11, PhMA; 12, 1PhEMA; 13, 2PhEMA; 14, FFMA; 15, MA; 16, EA; 17, BA; 18, BzA; 19, 2ClEA; 20, VAc; 21, VB; 22, VPAc; 23, VClAc; 24, AN; 25, αMAN; 26, MA(2Cl); 27, o-ClSt; 28, p-FSt; 29, o,p-FSt

refractive index; A, acrylate; XA, acrylate with high refractive index; Ac, vinyl acetate; XAc, vinyl acetate with high refractive index; C, acrylonitrile; α-A, α-substituted acrylate; St, styrene. The refractive-index profile of the GI POF was tightly controlled by copolymerizing two or three specific kinds of monomers in *Table 1* according to the following concepts.

Binary monomer system

In order to obtain the graded index effectively by our copolymerization procedure, two monomers (M_1 and M_2) satisfying the following conditions should be selected:

$$r_{12} > 1 \quad \text{and} \quad r_{21} < 1 \tag{3}$$

Here M_1 monomer is first preferentially polymerized at any monomer feed composition. Therefore, when the refractive index (n_1) of M_1 homopolymer is lower than that (n_2) of M_2 homopolymer, a GI preform rod in which the refractive index decreases monotonically from the centre axis to the periphery of the rod is obtained, since the copolymer phase is formed from the inner wall of the tube.

Figure 1 shows a *Q–e* map of the monomers in *Table 1*. When MMA is selected as M_1 monomer, the regions ($r_{12} < 1$ and $r_{21} > 1$), ($r_{12} < 1$ and $r_{21} < 1$) and ($r_{12} > 1$ and $r_{21} < 1$) are demarcated by thick full curves. It is shown that all of the monomers in the A, XA, Ac and XAc groups in *Table 1* are situated in the region ($r_{12} > 1$ and $r_{21} < 1$) in (3). The monomers in the XA and XAc groups, which satisfy the condition $n_{12} < n_{21}$, are candidates for obtaining a GI preform rod where the refractive index gradually decreases from the centre axis to the periphery.

To prepare such a GI preform rod, we selected benzyl acrylate (BzA), vinyl benzoate (VB) and vinyl phenylacetate (VPAc) as the M_2 monomer, while the M_1 monomer was MMA. *Figure 2* shows representative refractive-index profiles of these GI preform rods prepared by the interfacial-gel copolymerization process at 70°C for 24 h. The symbols n_0 and n are the refractive

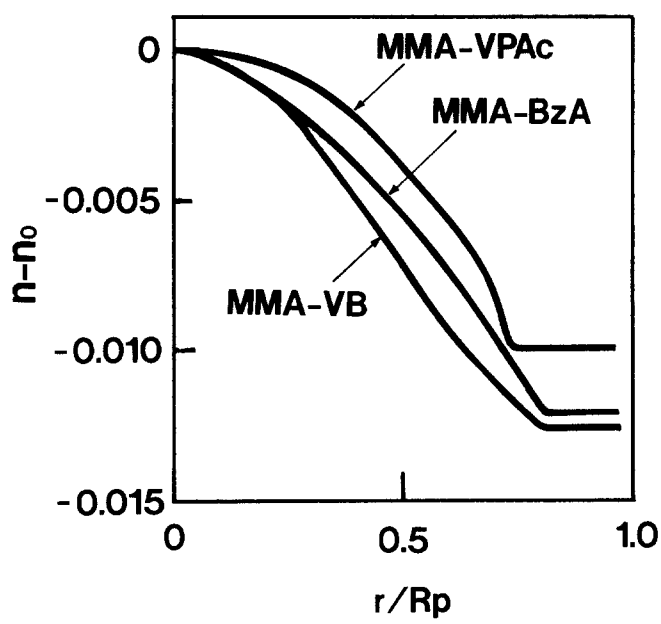

Figure 2 The refractive-index distribution of the GI preform rod prepared by the interfacial-gel copolymerization process. $M_1/M_2 = 4$ (wt/wt)

indices at the centre axis and at distance r from the centre axis, respectively, and R_p is the radius of the rod. Here the monomer feed ratio M_1/M_2 was 4.0 (wt/wt) and the amount of benzoyl peroxide (BPO) as initiator was 0.5 wt%. The amount of n-butylmercaptan (nBM) as chain-transfer agent was 0.15 wt% for MMA–VB and MMA–VPAc rods and 0 wt% for the MMA–BzA rod. All of the preform rods have cladding coming from the PMMA tube, and have quadratic index profiles at the core region.

Ternary monomer system

In the case of the above binary monomer system, the index distribution is limited to a profile where the refractive index decreases monotonically from the centre

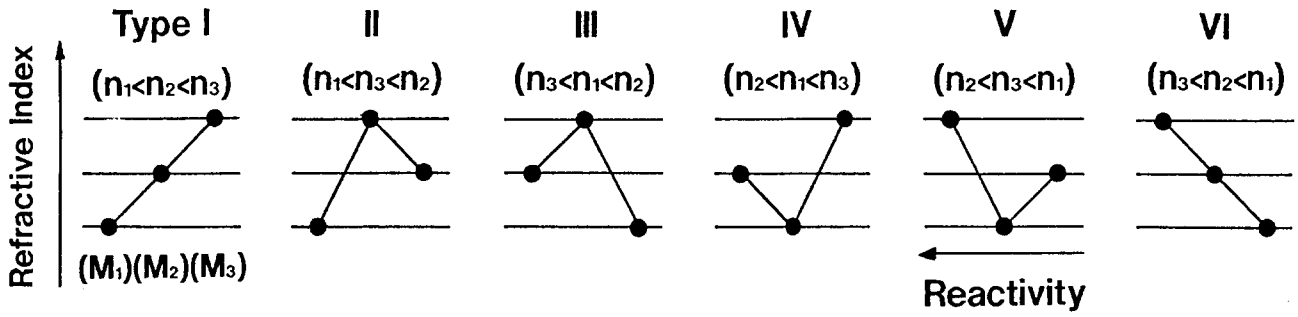

Figure 3 Classification of ternary monomer system

axis to the periphery. On the other hand, a specific ternary monomer system enables preparation of a GI fibre with a W-shaped index profile, where the refractive index decreases parabolically from the centre axis to an intermediate distance r_c and increases from r_c to the radius R_p of the fibre. In this fibre, light injected into the periphery region from r_c to R_p is gradually bent to the outside owing to the index profile, and does not pass through the fibre. On the other hand, light injected into the centre region within the numerical aperture (NA) of the fibre is transmitted along the fibre with a sinusoidal trajectory and with little modal dispersion. Therefore the regions inside and outside of r_c correspond to the core and cladding of the optical fibre, respectively.

In an SI polymer fibre, the transmission of light along the fibre relies on total internal reflection at the interface between the core and cladding. So when the core and cladding materials are not perfectly in contact at a smooth cylindrical interface, a serious scattering loss would occur. On the other hand, in the W-shaped index distribution, since there is no sharp boundary between the core and cladding, the light transmitted along the fibre has no reflection at the wall and a low-loss polymer optical fibre would be expected.

Now, we select the ternary monomer system satisfying the following conditions:

$$\begin{array}{lll} r_{12} > 1 & r_{13} > 1 & r_{23} > 1 \\ r_{21} < 1 & r_{31} < 1 & r_{32} < 1 \end{array} \qquad (4)$$

which indicates that an M_1-richer terpolymer is formed in the initial stage of copolymerization, an M_2-richer terpolymer in the intermediate stage and an M_3-richer terpolymer in the final stage. Since the copolymer phase is formed from the inner wall of the tube, M_1-richer terpolymer is placed in the periphery region of the GI preform rod, M_2-richer terpolymer in the intermediate region and M_2-richer terpolymer in the centre region.

Concerning the refractive index of each homopolymer, the ternary monomer system was classified into six types (types I–VI) as shown in *Figure 3*. Each triplet of points in *Figure 3* indicates M_1, M_2 and M_3 homopolymers from the left side, respectively. The ordinate expresses the refractive index of each homopolymer, and the abscissa indicates the reactivity of copolymerization, where the M_1 monomer is first preferentially polymerized according to the conditions in (4). Here types IV and V are candidates to obtain the W-shaped index profile, because the refractive indices (n_1, n_2 and n_3) of the M_1, M_2 and M_3 homopolymers, respectively, are $n_2 < n_1 < n_3$ in type IV and $n_2 < n_3 < n_1$ in type V. Namely, in both types, n_2 is the lowest among them, so that the M_2-richer terpolymer placed in the intermediate region has the lowest refractive index, forming a minimum peak of the index distribution at the distance r_c.

Table 2 Possible ternary monomer combinations for W-shaped GI POF of type IV

Combination of monomer group	Number	Example
XMA–(A, MA, C, A c, S t)–XAc	22	BzMA,PhMA–BA–VB
	10	PhMA–iPMA–VB
	9	PhMA–AN–VB
	3	2PhEMA–VAc–VPAc
	1	PhMA–o,p-FSt–VB
XMA–(A, MA)–XA	4	FFMA,1PhEMA–EA–BzA
	1	FFMA–nPMA–BzA
α-A–(MA, A, C, S t, A C)–XAc	34	MAtro–MMA,EMA,iPMA–VPAc
	12	MAtro–EA–VPAc
	4	MAtro–αMAN–VB
	4	MAtro–o,p-FSt–VB
	2	MA(2Cl)–VAc–VPAc
α-A–(MA, A, S t, MA, A)–(XA, C)	16	MA(2Cl)–EMA–BzA,2ClEA
	3	MA(2Cl)–MA–BzA
	2	MA(2Cl)–o,p-FSt–BzA,2ClEA
	9	MA(2Cl)–TBMA–AN
	1	MA(2Cl)–EA–AN
C–(A, MA, A c)–XAc	6	αMAN–BA–VPAc
	2	αMAN–nPMA–VPAc
	2	AN–VAc–VPAc
C–(A, MA, MA, A)–(XA, C)	2	αMAN–EA–BzA
	1	αMAN–nPMA–BzA
	1	αMAN–nPMA–AN
	1	αMAN–EA–AN
St–(A, MA, C, Ac, S t)–XAc	8	p-FSt–BA–VB
	2	p-FSt–nPMA–VB
	2	p-FSt–AN–VB
	2	p-iPSt–VAc–VPAc
	2	p-FSt–p,o-FSt–VB
MA–(A, A c, A, A)–(XAc, XA, C)	23	MMA–BA–VPAc,VB
	2	CHMA–VAc–VPAc
	6	CHMA–EA–BzA
	2	CHMA–EA–AN
XA–A c–XAc	2	2ClEA–VAc–VPAc

The possible combinations of ternary monomers belonging to types IV and V were selected from the monomers in *Table 1*, and are listed in *Tables 2* and *3*. All combinations of ternary monomer groups categorized in *Table 1* are listed on the left side, and the numbers in the centre column indicate the possible number of monomer combinations. Examples of the ternary monomer combination in each line are listed on the right-hand side. It is noteworthy that there are so many

Table 3 Possible ternary monomer combinations for W-shaped GI POF of type V

Combination of monomer group	Number	Example
A, MA, C, A c, S t → XMA, XAc	20	BzMA,PhMA–MA–VPAc
	19	BzMA–MMA–VPAc
	3	PhMA–AN–VPAc
	2	BzMA–VAc–VPAc
	2	PhMA–o,p-FSt–VPAc
MA, A, S t, C → XMA, XA	19	BzMA,PhMA–MMA–VPAc,VClAc
	9	PhMA–EA–BzA
	2	PhMA–o,p-FSt–2ClEA
	1	PhMA–αMAN–BzA
MA, A → XMA, C	10	PhMA–tBMA–AN
	4	2PhEMA–EA–AN
MA, A, S t → α-A, XAc	18	MAtro–nBMA–VClAc
	5	MAtro–EA–VClAc
	2	MAtro–o,p-FSt–VClAc
MA, A, S t, C → α-A, XA	18	MAtro–tBMA–BzA
	3	MAtro–EA–BzA
	2	MAtro–o,p-FSt–BzA
	1	MAtro–αMAN–BzA
MA, A → α-A, C	9	MAtro–EMA–AN
	1	MAtro–EA–AN
A, MA, A, MA → C, XAc, XA	3	αMAN–BA–VClAc
	1	αMAN–nPMA–VClAc
	1	αMAN–EA–2ClEA
	1	αMAN–nPMA–2ClEA
MA, A, S t, C, A c → St, XAc	28	o-ClSt–MMA–VB
	12	o-ClSt–EA–VPAc
	7	o-ClSt–o,p-FSt–VClAc
	2	o-ClSt–AN–VPAc
	1	o-ClSt–VAc–VPAc
MA, A, S t, MA, A → St, XA, C	20	o-ClSt–nPMA–BzA
	6	o-ClSt–MA–BzA
	3	o-ClSt–o,p-FSt–2ClEA
	10	o-ClSt–nBMA–AN
	2	o-ClSt–EA–AN

combinations of ternary monomers satisfying the condition of types IV and V to obtain a W-shaped GI fibre. *Figure 4* shows a representative index distribution of the W-shaped GI preform rod prepared by the photocopolymerization of BzMA–VAc–VPAc monomer system.

LIGHT SCATTERING AND HETEROGENEITY OF COPOLYMER

Light-scattering analysis

A very slight amount of heterogeneity inside a GI polymer optical fibre causes a large effect on the light-scattering loss. The transmission loss through such a GI fibre is governed by the scattering loss, with an order of 100 dB km^{-1} in the visible region. It was theoretically and experimentally confirmed[14,15] that the inherent light-scattering loss of amorphous homopolymer glasses such as PMMA is of the order of 10 dB km^{-1} around the wavelength of red light, which is near to the theoretical limit estimated by the thermally induced density fluctuations in a structureless liquid. So, in copolymer glasses such as poly(MMA–VPAc) and poly(MMA–BzA), which are GI POF materials, the effect of the composition distribution of copolymer on the heterogeneous structure giving such excess light scattering should be considered further.

Poly(MMA–VPAc), poly(MMA–BzA) and poly(MMA–BzMA) rods were copolymerized at 130°C for 96 h with di-t-butyl peroxide (DBPO) of 0.3 wt% and nBM of 0.2 wt% to study the inherent light scattering of these copolymers. The monomer mixture was carefully purified according to our previous paper[14], and was slowly distilled into a glass ampoule, sealed under vacuum and immersed in silicone oil for polymerization. After polymerization the resulting copolymer rod with 20 mm diameter was taken out of the ampoule for measurement of light scattering. Since thermal copolymerization was carried out homogeneously in an ampoule, no index distribution exists inside these copolymer rods.

The sample rod was placed vertically at the centre of the goniometer and a He–Ne laser beam was injected from the side; the scattered light from the centre region of the rod was detected. The polarized (Vv) and depolarized (Hv) light scattering intensities were measured, the details of which were described elsewhere[14]. The result of measurements on these copolymer rods is shown in *Figure 5*. It is quite interesting that, although the Hv intensity was independent of the scattering angle for all samples and was $\sim 10^{-6}$ cm^{-1}, the Vv intensity increased with decreasing scattering angle θ. This angular dependence of Vv suggests the existence of large-sized heterogeneities with a dimension of more than several hundred ångströms. On the other hand, since Hv intensity had no angular dependence, it is suggested that these heterogeneous structures are isotropic and no nodular structures such as anisotropic ordering of molecules exist. In randomly oriented polymer bulk, the isotropic part Vv^{iso} of Vv is given by[16]:

$$Vv^{iso} = Vv - \tfrac{4}{3}Hv \quad (5)$$

Therefore, we divided Vv in *Figure 5* into three terms, Vv_1^{iso}, Vv_2^{iso} and $\frac{4}{3}Hv$. Namely:

$$Vv = (Vv_1^{iso} + Vv_2^{iso}) + \tfrac{4}{3}Hv$$

where Vv_1^{iso} denotes the isotropic background scattering independent of the scattering angle, and Vv_2^{iso} is the isotropic scattering that depends on the scattering angle due to large-sized heterogeneities. Finally, the total scattering loss α_t (dB km^{-1}) is obtained, as shown in ref.

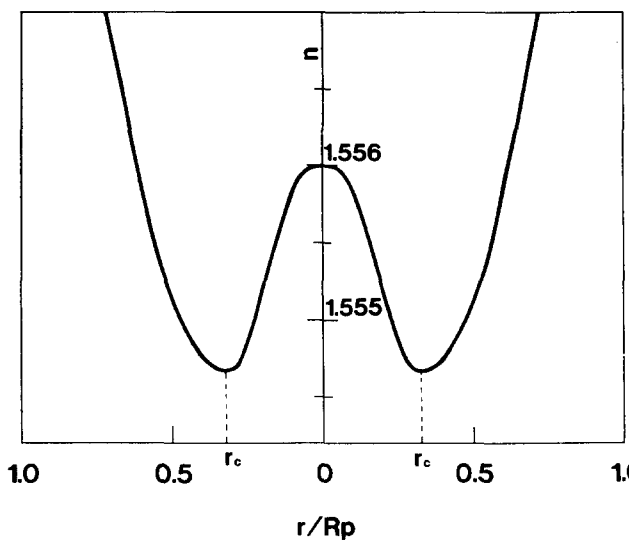

Figure 4 The index distribution of the W-shaped GI preform rod prepared by the photocopolymerization of BzMA–VAc–VPAc monomer system

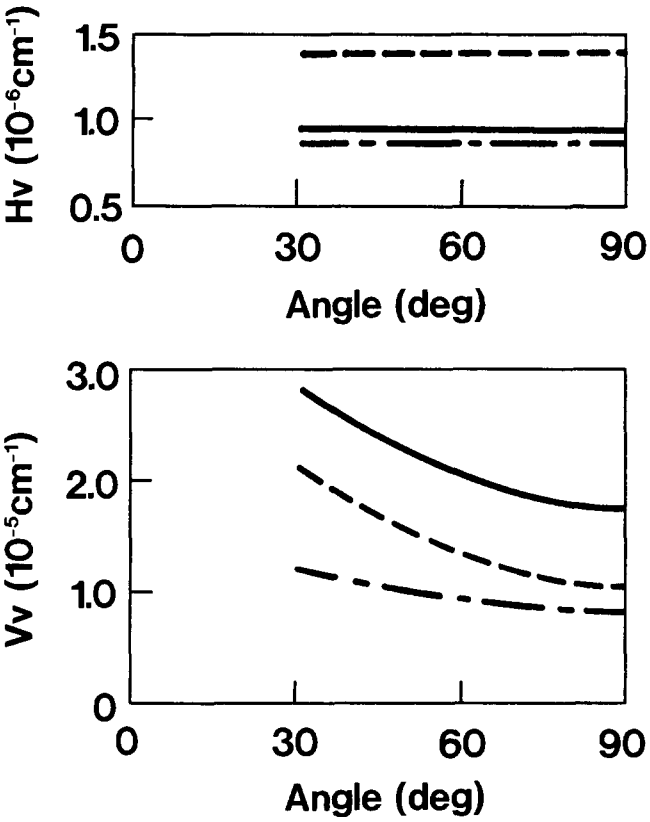

Figure 5 Hv and Vv scatterings of the copolymer glass of $M_1/M_2 = 4$ (wt/wt): (———), MMA–VPAc; (---), MMA–BzA; (-·-), MMA–BzMA

14, by equation (6), where Vv_1^{iso}, Vv_2^{iso} and Hv have the unit of cm^{-1}:

$$\alpha_t = 1.36 \times 10^6 \int_0^{\pi} [(1 + \cos^2\theta)(Vv_1^{iso} + Vv_2^{iso}) + (13 + \cos^2\theta)Hv/3] \sin\theta \, d\theta \quad (6)$$

Here, α_t is divided into three terms, α_1^{iso}, α_2^{iso} and α^{aniso}. That is:

$$\alpha_t = \alpha_1^{iso} + \alpha_2^{iso} + \alpha^{aniso}$$

where α_1^{iso} is the isotropic scattering loss from Vv_1^{iso} with no angular dependence, α_2^{iso} is the isotropic scattering loss from Vv_2^{iso} due to large-sized heterogeneities and α^{aniso} is the anisotropic scattering loss from Hv.

Table 4 shows these scattering parameters for the copolymer samples. Details of the estimation method from Vv and Hv intensities have been given elsewhere[14]. The molecular weight (M_w weight average; M_n number average), glass transition temperature T_g and remaining monomer for these samples are listed in *Table 5*. It is noteworthy that the total scattering losses α_t of these samples are 35–70 dB km^{-1} and are competitive with those of homopolymers. The large value of α^{aniso} ($\sim$10 dB km^{-1}) compared with that of the PMMA homopolymer glass ($\sim$5 dB km^{-1})[14] could mainly be attributed to the anisotropy of the phenyl groups of monomer units. The α_2^{iso} could be caused by the large-sized heterogeneities due to the density fluctuation and/or the distribution of the copolymer composition.

Effect of local structure of copolymer on light scattering

Since the angular independence of Hv in *Figure 5* showed the random orientation, Debye's theory[17] written as equation (7) may be adopted:

$$Vv_2^{iso} = \frac{4\langle\eta^2\rangle\pi^3}{\lambda_0^4} \int_0^{\infty} \frac{\sin(vsr)}{vsr} r^2\gamma(r)\,dr \quad (7)$$

with

$$v = 2\pi n/\lambda_0 \qquad s = 2\sin(\theta/2)$$

Here $\langle\eta^2\rangle$ denotes the mean-square average of the fluctuation of all dielectric constants, λ_0 is the wavelength of light in vacuum and n is the refractive index of the sample. $\gamma(r)$ refers to the correlation function defined by $\eta_i\eta_j/\langle\eta^2\rangle$ where η_i and η_j are the fluctuations of dielectric constants at i and j positions. In this paper, the correlation function $\gamma(r)$ is assumed to be approximated by equation (8) as suggested by Debye *et al.*[17]:

$$\gamma(r) = \exp(-r/a) \quad (8)$$

where a is called the correlation length and is a measure of the size of the heterogeneities. Substituting equation (8) into equation (7) and integrating gives:

$$Vv_2^{iso} = \frac{8\pi^3\langle\eta^2\rangle a^3}{\lambda_0^4(1 + v^2s^2a^2)^2} \quad (9)$$

The arrangement of equation (9) gives the Debye plot[17], where $(Vv_2^{iso})^{-1/2}$ *versus* s^2 shows a straight line, and the correlation length a can be determined by $a = (\lambda/2\pi)(\text{slope/intercept})^{1/2}$. The values of a and $\langle\eta^2\rangle$ obtained by this method are listed in *Table 4*. It is confirmed that the scattering α_2^{iso} of 16.6–17.9 dB km^{-1} is caused by heterogeneities with correlation length a of 350–600 Å and $\langle\eta^2\rangle$ of 6×10^{-9}–1.5×10^{-8}. If it is assumed that these heterogeneities consist of two phases in which each volume fraction is ϕ_1 and ϕ_2, and the refractive indices are n_1 and n_2, respectively, then a and $\langle\eta^2\rangle$ are given by[17]:

$$a = (4V/S)\phi_1\phi_2 \quad (10)$$

$$\langle\eta^2\rangle \simeq \phi_1\phi_2(n_1^2 - n_2^2)^2 \simeq 4\phi_1\phi_2 n^2(\Delta n)^2 \quad (11)$$

where S is the total surface area of the boundary between the two phases, V is the total volume, n is the average refractive index, Δn is $(n_1 - n_2)$ and $\phi_1 + \phi_2 = 1$. Equation (10) indicates that if the boundary surface between

Table 4 Scattering parameters of the copolymer glasses. $M_1/M_2 = 4$ (wt/wt)

Polymer sample M_1–M_2	$\langle\eta^2\rangle$ ($\times 10^{-9}$)	a (Å)	α_1^{iso} (dB km^{-1})	α_2^{iso} (dB km^{-1})	α^{aniso} (dB km^{-1})	α_t (dB km^{-1})
MMA–VPAc	10.9	397	43.1	16.6	10.5	70.2
MMA–BzA	6.0	594	18.0	17.9	16.9	52.8
MMA–BzMA	15.1	344	8.3	17.2	10.1	35.6

Table 5 Physical properties of copolymer glasses in *Table 4*

Polymer sample M_1–M_2	M_w ($\times 10^4$)	M_n ($\times 10^4$)	M_w/M_n	T_g (°C)	Remaining monomer: MMA (wt%)	Remaining monomer: M_2 (wt%)
MMA–VPAc	14.6	6.2	2.36	75.4	0	4.38
MMA–BzA	15.4	9.4	1.64	71.1	0.71	0.14
MMA–BzMA	6.0	2.6	2.27	97.5	0	0.42

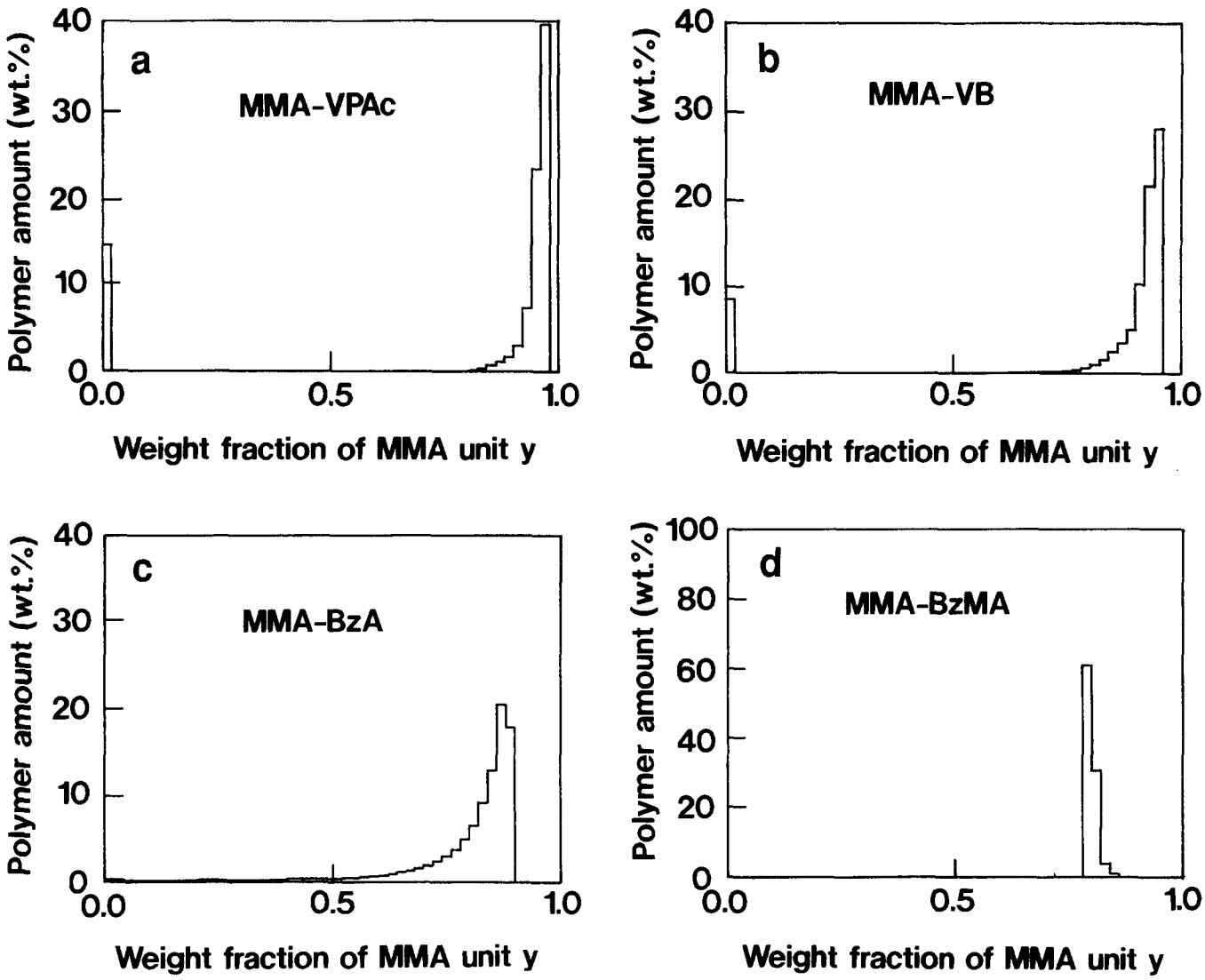

Figure 6 Distribution of copolymer composition after 100% polymerization when $M_1/M_2 = 4$ (wt/wt)

the two phases is intricate, the value of S increases to give a smaller value of the correlation length. Equation (11) shows that if $\phi_1 = 0.1$–0.9, the fluctuation of the refractive index is the order of 10^{-5}.

As the origin of these heterogeneities inside the copolymer glasses, we should also investigate the effect of the distribution of copolymer composition. If it is assumed that the monomer reactivity ratios r_{12} and r_{21} are constants during polymerization, the monomer conversion P (weight fraction) is related to the weight fraction (x) of the M_1 monomer in the remaining monomer mixture by[18]:

$$P = 1 - \left(\frac{x}{x_0}\right)^{\alpha}\left(\frac{x-1}{x_0-1}\right)^{\beta}\left(\frac{x-k}{x_0-k}\right)^{\gamma} \qquad (12)$$

with

$$\alpha \equiv \frac{r_2}{1-r_2} \qquad \beta \equiv \frac{r_1}{1-r_1}$$

$$\gamma \equiv \frac{r_1 r_2 - 1}{(1-r_1)(1-r_2)}$$

$$k \equiv \frac{w(1-r_2)}{w(1-r_2)+(1-r_1)}$$

Here x_0 is the weight fraction of the M_1 monomer in the monomer feed, and w is the ratio of molecular weights of monomers M_1 to M_2. The rearranged form of the Mayo–Lewis equation using units of weight fraction is:

$$y = \frac{(r_1 - w)x^2 + wx}{[w(r_2 - 1) + r_1 - 1]x^2 - (2r_2 w - w - 1)x + r_2 w} \qquad (13)$$

where y is the instantaneous weight fraction of M_1 unit in the copolymer. Since $-dP/dy$ expresses the amount of copolymer having composition y, the curve of $-dP/dy$ *versus* y represents the composition distribution of the copolymer formed. If r_2 is less than 0.5, which is the case for the MMA–VPAc monomer system, MMA monomer is consumed during polymerization and only M_2 homopolymer is formed at the final stage of the polymerization[18]. Namely, $-dP/dy$ becomes infinite when y reaches zero. Therefore, in order to avoid this inconvenience, the increment of the conversion, ΔP, for each $\Delta y = 0.02$ is calculated against the copolymer composition y.

The histogram when calculated at $M_1/M_2 = 4$ (wt/wt) is shown in *Figure 6*, which corresponds to the copolymer composition after completing polymerization, and the relevant values of r_{12} and r_{21} are listed in *Table 6*. In the case of MMA–VPAc and MMA–VB copolymers, the distribution of the copolymer composition is mainly

Table 6 Monomer reactivity ratios

M_1–M_2	r_{12}	r_{21}
MMA–VPAc	22.5	0.005
MMA–VB	8.52	0.07
MMA–BzA	2.53	0.31
MMA–BzMA	0.93	1.05

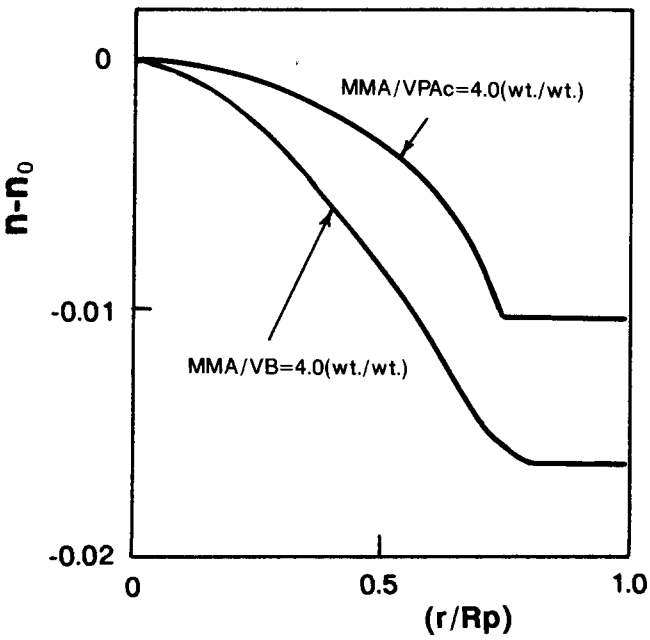

Figure 7 The refractive-index distribution of the GI POF with a 0.6 mm diameter

divided into two compositions because $r_2 \ll 0.5$. One is the composition that is formed in the initial stage of polymerization and is quite similar to that of PMMA. The other is the composition that is formed in the final stage of polymerization and is almost M_2 homopolymer. Therefore, we can say that the compositions of poly(MMA–VPAc) and poly(MMA–VB) are similar to blend polymers. In the case of MMA–BzA, r_2 is near to 0.5, and little BzA homopolymer may be formed compared with the case of poly(MMA–VB) and poly(MMA–VPAc). On the other hand, poly(MMA–BzMA) may have a very monodisperse distribution of composition as shown in *Figure 6* because $r_1 \simeq r_2 \simeq 1$.

It is noted that the total scattering losses α_t of poly(MMA–VPAc), poly(MMA–BzA) and poly(MMA–BzMA) decreased, in turn, as 70.2, 52.8 and 35.6 dB km^{-1}, as shown in *Table 4*. This result may imply a correlation between scattering loss and the heterogeneity of the composition distribution. Concerning the scattering loss, MMA–BzA is better than MMA–VPAc, but MMA–BzA GI preform had a slight amount of crosslinkage[19] probably due to the unstable α-hydrogen of the BzA monomer and could not be heat-drawn into GI POF.

If it is assumed that the MMA-like and VPAc-like polymer molecules in poly(MMA–VPAc) are phase-separated from each other, then Δn in equation (11) should be estimated as the difference between the refractive indices of MMA and VPAc homopolymers, i.e. $\Delta n = 0.07$, and the calculated $\langle \eta^2 \rangle$ becomes 7×10^{-3}. This value is approximately five orders of magnitude larger than the observed $\langle \eta^2 \rangle$ of poly(MMA–VPAc) in *Table 4*. The solubility parameters of the MMA and VPAc homopolymers are 9.3 and 10.0 (cal $cm^{-3})^{1/2}$, respectively, and nearly equal, so there is a possibility that the MMA-like and VPAc-like polymers would be mixed without such phase separation. However, the poly(MMA–VPAc) sample in *Table 5* still includes the remaining monomer of 4 wt%. A persuasive conclusion on this will be obtained when perfectly polymerized poly(MMA–VPAc) glass is obtained.

PROPERTIES OF GRADED-INDEX POLYMER OPTICAL FIBRE

The refractive-index distribution of the GI POF was measured by the transverse interferometric technique[20]. The refractive-index distributions of the MMA–VPAc and MMA–VB fibres prepared by the interfacial-gel copolymerization process are shown in *Figure 7*. The preform rods ($M_1/M_2 = 4.0$ (wt/wt)) were prepared at 70°C for 24 h with BPO = 0.5 wt% and nBM = 0.2 wt%. The normalized index distributions of these fibres are almost the same as those of the preform rods. The numerical apertures (NA) estimated from the index difference of the gradient index are 0.18 and 0.22 for the MMA–VPAc and MMA–VB fibres, respectively.

The total attenuation spectrum of the light transmission through the GI POF was measured by using a spectrum analyser (Advantest Co., model TQ8345). The results for the GI POF of *Figure 7* are shown in *Figure 8*. The total attenuations, at 652 nm, were 143 and 134 dB km^{-1} for the MMA–VPAc and MMA–VB fibres, respectively. It should be noted that these values are comparable with the attenuation (100–300 dB km^{-1}) of commercially available SI POF. The dramatic decrease in the attenuation compared with our published data[21] in the photocopolymerization process could be attributed to a smooth boundary between the core and cladding by the new interfacial-gel copolymerization process.

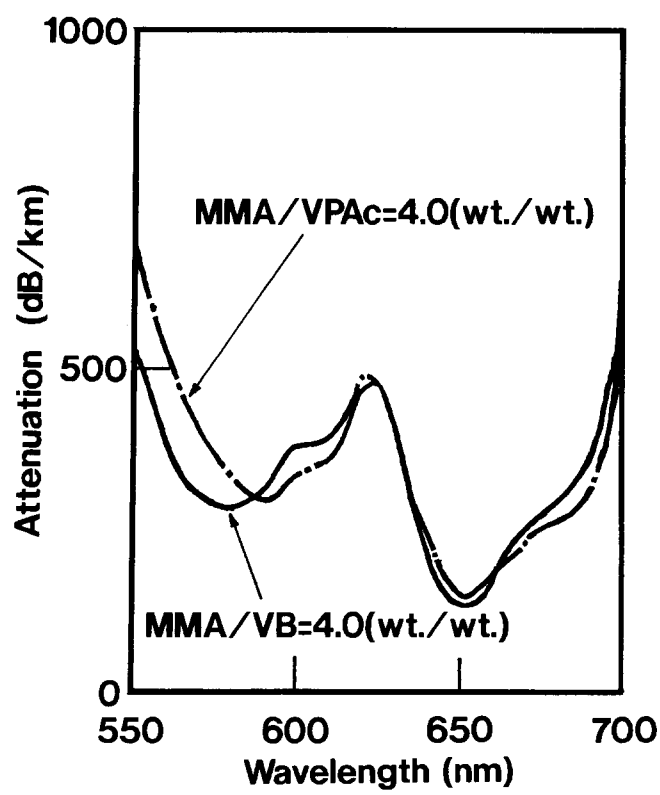

Figure 8 The total attenuation through the GI POF

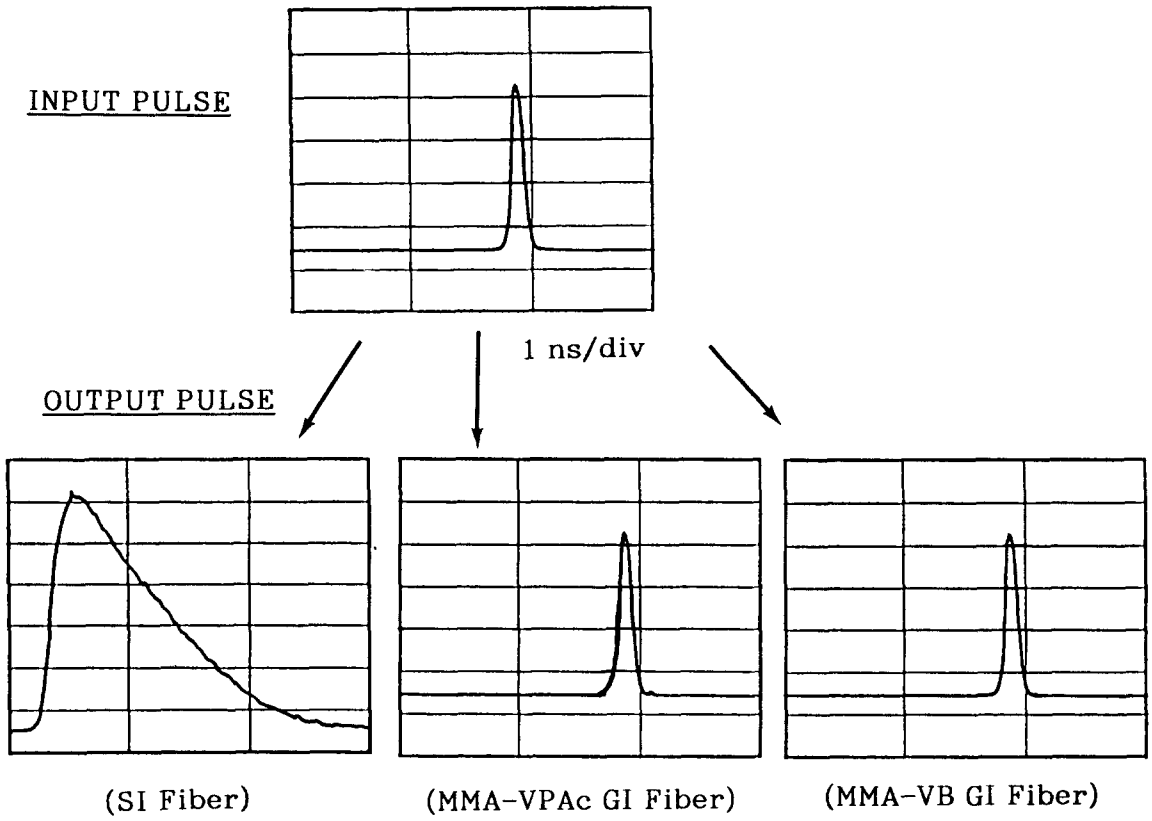

Figure 9 Bandwidth measurement by spreading of the output pulse through 15 m fibre

The bandwidth of the GI and SI POFs was measured as follows. A pulse of 10 MHz from an InGaAlP laser diode (wavelength = 670 nm) was injected ($NA = 0.5$) into a 15 m long fibre. The output pulse was detected by a sampling head (model 00S-01, Hamamatsu Photonics Co.). The results for the MMA–VPAc and MMA–VB GI POF in *Figure 7* are shown in *Figure 9*, compared with the SI POF[7]. It is quite noteworthy that, although the output pulse through the SI POF is quite spread, the pulse through the GI POF is almost the same as the input pulse. The bandwidth of the SI POF estimated at the 3 dB level in the pulse response function is 6 MHz km, while the bandwidths of the MMA–VPAc and MMA–VB GI POFs in *Figure 9* are 125 and 260 MHz km, respectively. The excellent bandwidth of the GI POF compared with the conventional SI POF was experimentally confirmed even for short-distance communication.

The tensile strength of the GI POF was measured by elongating a 100 mm length of POF at a rate of 100 mm min^{-1}. Both MMA–VPAc and MMA–VB GI POFs are very flexible and the tensile strengths at the yield point are 400–700 kg cm^{-2}, which are comparable to those of commercially available SI POFs.

CONCLUSIONS

A low-loss and high-bandwidth GI POF with good mechanical properties was successfully obtained by utilizing the difference in monomer reactivities. Although the binary monomer system gave only an index distribution in which the refractive index decreased monotonically from the centre axis to the periphery, the ternary monomer system gave a W-shaped index distribution with many possible ternary monomer combinations, as shown in *Tables 2* and *3*.

The dependence of the light-scattering loss on the composition distribution of the copolymer core materials was quantitatively confirmed by the angular dependence of the Vv scattering. It is noted that the total scattering losses of the GI core materials are 35–70 dB km^{-1} and are competitive with those of homopolymers.

It is experimentally demonstrated that the GI POF is quite superior to the conventional SI POF in the bandwidth, while the attenuations of both POFs are comparable.

REFERENCES

1 Kaino, T. *J. Polym. Sci.(A)* 1987, **25**, 37
2 Koike, Y., Nihei, E., Tanio, N. and Ohtsuka, Y. *Appl. Opt.* 1990, **29**, 2686
3 Emslie, C. *J. Mater. Sci.* 1988, **23**, 2281
4 Groh, W., Lupo, D. and Sixl, H. *Angew. Chem., Int. Edn Engl., Adv. Mater.* 1989, **28**, 1548
5 Sorm, M. *Tech. Mod.* 1988, **80**, 19
6 Scholl, F. W., Coden, M. H., Anderson, S. and Dutt, B. Proc. FOC/LAN '88, 1988, p. 338
7 Eska series, Mitsubishi Rayon Co. Ltd
8 Toray plastic optical fibre PF/PG series
9 Ohtsuka, Y. and Koike, Y. *Appl. Opt.* 1984, **23**, 1774
10 Koike, Y., Hatanaka, H. and Ohtsuka, Y. *Appl. Opt.* 1984, **23**, 1779
11 Ohtsuka, Y. and Koike, Y. *Appl. Opt.* 1985, **24**, 4316
12 Koike, Y., Takezawa, Y. and Ohtsuka, Y. *Appl. Opt.* 1988, **27**, 486
13 Koike, Y., Tanio, N., Nihei, E. and Ohtsuka, Y. *Polym. Eng. Sci.* 1989, **29**, 1200
14 Koike, Y., Tanio, N. and Ohtsuka, Y. *Macromolecules* 1989, **22**, 1367
15 Tanio, N., Koike, Y. and Ohtsuka, Y. *Polym. J.* 1989, **21**, 259
16 Meeten, G. H. 'Optical Properties of Polymers', Elsevier Applied Science, London, 1986
17 Debye, P., Anderson, H. R. and Brumberger, H. *J. Appl. Phys.* 1957, **28**, 679
18 Meyer, V. E. and Lowry, G. G. *J. Polym. Sci. (A)* 1965, **3**, 2843
19 Cameron, G. C. and Kane, D. R. *Polymer* 1968, **9**, 461
20 Koike, Y., Sumi, Y. and Ohtsuka, Y. *Appl. Opt.* 1986, **25**, 3356
21 Koike, Y., Kimoto, Y. and Ohtsuka, Y. *Appl. Opt.* 1982, **21**, 1057